

PAPER

Ambipolar transport and magneto-resistance crossover in a Mott insulator, Sr_2IrO_4

To cite this article: J Ravichandran *et al* 2016 *J. Phys.: Condens. Matter* **28** 505304

View the [article online](#) for updates and enhancements.

You may also like

- [Testing the Strong Equivalence Principle. II. Relating the External Field Effect in Galaxy Rotation Curves to the Large-scale Structure of the Universe](#)
Kyu-Hyun Chae, Harry Desmond, Federico Lelli et al.
- [Numerical Solutions of the External Field Effect on the Radial Acceleration in Disk Galaxies](#)
Kyu-Hyun Chae and Mordehai Milgrom
- [The Global Stability of M33 in MOND](#)
Indranil Banik, Ingo Thies, Benoit Famaey et al.

Ambipolar transport and magneto-resistance crossover in a Mott insulator, Sr_2IrO_4

J Ravichandran^{1,4}, C R Serrao², D K Efetov^{1,5}, D Yi^{2,6}, Y S Oh³, S-W Cheong³, R Ramesh² and P Kim^{1,7}

¹ Department of Physics, Columbia University, New York, NY 10027, USA

² Department of Materials Science and Engineering, University of California, Berkeley, CA 94720, USA

³ Rutgers Center for Emergent Materials and Department of Physics and Astronomy, Piscataway, NJ 08854, USA

E-mail: jayakanr@usc.edu and pkim@physics.harvard.edu

Received 27 August 2016, revised 28 September 2016

Accepted for publication 13 October 2016

Published 28 October 2016



Abstract

Electric field effect (EFE) controlled magnetoelectric transport in thin films of undoped and La-doped Sr_2IrO_4 (SIO) is investigated using ionic liquid gating. The temperature dependent resistance measurements exhibit insulating behavior in chemically and EFE doped samples with the band filling up to 10%. The ambipolar transport across the Mott gap is demonstrated by EFE tuning of the channel resistance and chemical doping. We observe a crossover from high temperature negative to low temperature positive magnetoresistance around ~ 80 – 90 K, irrespective of the filling. This temperature and magnetic field dependent crossover is discussed in the light of conduction mechanisms of SIO, especially variable range hopping (VRH), and its relevance to the insulating ground state of SIO.

Keywords: Mott insulator, ionic liquid gating, thin film, magnetoresistance, hopping conduction, iridate

(Some figures may appear in colour only in the online journal)

1. Introduction

Transition metal oxides (TMOs) are excellent model systems for Mott insulators, where localized d -orbitals cause strong electron correlation effects [1, 2]. As we move down the periodic table, from $3d$ to $5d$, TMOs show weaker electron correlation but larger spin–orbit coupling, due to higher atomic numbers. Among the $5d$ TMOs, Ruddlesden–Popper series of iridates such as $\text{Sr}_{n+1}\text{Ir}_n\text{O}_{3n+1}$ ($n > 0$), specifically Sr_2IrO_4

(SIO), show an unusually robust insulating ground state, which persists despite chemical doping and applied pressure [3, 4]. The nature and origin of this insulating nature of SIO remains controversial [5–9]. To resolve this issue, there have been a few investigations into electron transport mechanisms in SIO [3, 10–15], but more studies are needed to unravel the intricate relationships between the role of disorder and transport mechanisms of the insulating state. This compound also shows a weak ferromagnetic moment [10], attributed to its canted antiferromagnetic ground state [16–18]. Recent magneto-transport measurement suggested a thickness dependent crossover behavior from Mott variable range hopping (VRH) to Efros–Shklovskii (ES) VRH for the low temperature conduction mechanism [13], indicating the importance of disorder in the sample. Due to the interplay between electron correlation, spin–orbit coupling, magnetism, crystal field effects and disorder, understanding the nature of insulating state in SIO

⁴ Present address: Mork Family Department of Chemical Engineering and Materials Science, University of Southern California, Los Angeles, CA 90089, USA.

⁵ Present address: Department of Electrical Engineering, Massachusetts Institute of Technology, Cambridge, MA 02139, USA.

⁶ Present address: Department of Applied Physics, Stanford University, Stanford, CA 94305, USA.

⁷ Present address: Department of Physics, Harvard University, Cambridge, MA 02138, USA.

remains complicated and yet interesting. Moreover, predictions of superconductivity in the electron doped SIO and its similarities to La_2CuO_4 [19], invites a thorough transport study to identify a route to achieve metallicity in Mott insulating SIO.

Electric field effect (EFE) [20] is a powerful tool to study the effect of band filling on transport properties, without creating doping induced disorder. In particular, recent progress in the use of ionic liquids for electrostatic modification of surfaces [21–24] has extended the limits of EFE doping close to $\sim 10^{15} \text{ cm}^{-2}$. This method has enabled experimental probing of a wide range of the electron density dependent phase diagrams [23, 24] and phases inaccessible by chemical doping [22]. Thus, EFE doping with ionic liquids provides a good experimental platform to explore the electronic phase diagram of the Mott insulators without significant chemically induced disorder. In a recent experiment [15], Lu *et al* demonstrated electrolyte gate induced modulation of magneto-transport in undoped SIO, suggesting the intimate coupling of charge, orbital, and spin degrees of freedom in this oxide.

In this article, we study the transport mechanisms in SIO using magnetoresistance (MR) measurements combined with electrolyte gating on undoped and La-doped thin films of SIO (5% La– $\text{La}_{0.05}\text{Sr}_{1.95}\text{IrO}_4$ and 10% La– $\text{La}_{0.1}\text{Sr}_{1.9}\text{IrO}_4$) and their corresponding magnetic properties. We measured magnetotransport under ionic liquid gating for the chemically undoped samples, where an ambipolar transport characteristics is observed. We found that the low temperature transport is always dominated by variable range hopping (VRH) accompanied by a MR crossover at ~ 80 – 90 K, both irrespective of the band filling. The magnetization measurements show a small spontaneous magnetization developing at ~ 240 K and ~ 150 K for nominally undoped SIO and $\text{La}_{0.1}\text{Sr}_{1.9}\text{IrO}_4$. We discuss these results to throw some light into the transport mechanisms in SIO.

2. Experimental methods

Thin films of SIO (10–25 nm thick) were grown epitaxially on $(\text{LaAlO}_3)_{0.3}(\text{Sr}_2\text{AlTaO}_6)_{0.7}$ (LSAT) and SrTiO_3 (STO) substrates using pulsed laser deposition, as discussed elsewhere [25]. Detailed structural and chemical characterizations of these epitaxial films to demonstrate their quality have already been established [25]. The transport measurements were carried out in both Hall bar or van der Pauw device geometry. Electrodes for the samples and the side gate for electrolyte were fabricated using electron beam lithography with poly(methyl methacrylate) (PMMA) as the resist. Pd (10 nm)/Au (70 nm) contacts and side gate electrodes were deposited using electron beam metal evaporation. The films were then etched into Hall bar geometry, whose lateral size is $\sim 100 \mu\text{m}$, using Ar ion milling. A small drop of ionic liquid, N, N-diethyl-N-(2-methoxyethyl)-N-methylammonium bis (trifluoromethyl sulphonyl)-imide (DEME TFSI), was applied on to the device with the liquid covering the entire channel and the side gates working as a counter electrode (inset of figure 1(a)). AC Magnetization measurements were carried out in a Quantum Design MPMS.

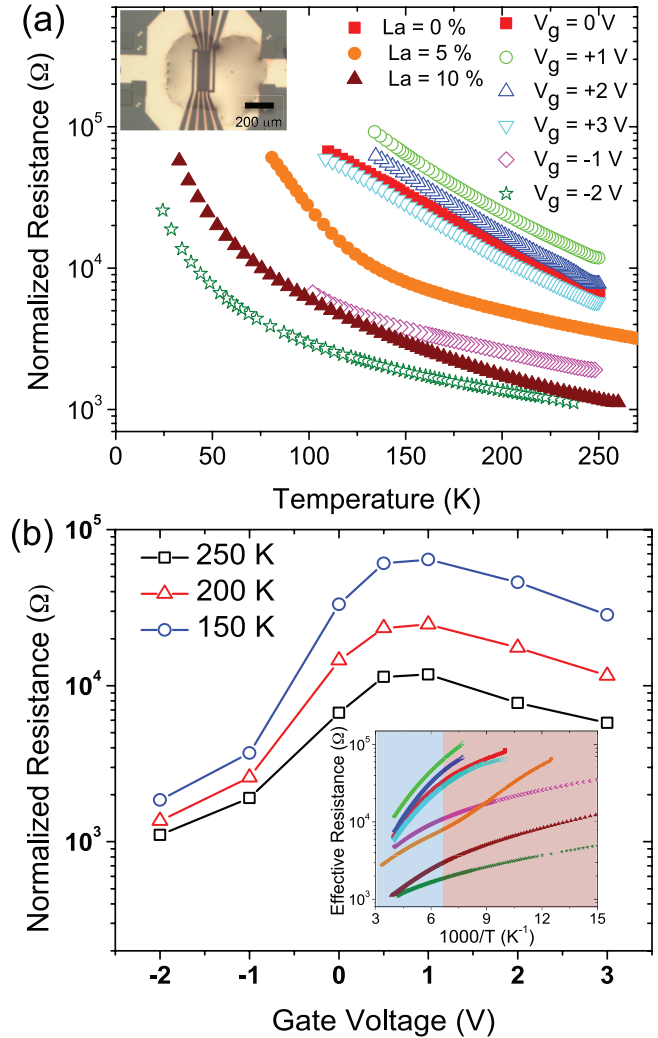


Figure 1. (a) Temperature dependent resistance of an undoped 10 nm thick SIO film with ionic liquid gating (for different applied gate voltages, V_g) and chemically doped films (5 and 10% La). The resistance values of chemically doped films were normalized to a 10 nm thick film for comparison. The inset shows the optical image of the Hall bar device of this 10 nm thick undoped SIO film with the ionic liquid. (b) The normalized resistances at 250 K (black open squares), 200 K (red open triangles), and 150 K (blue open circles) are shown as a function of V_g . The inset shows the semilog plot of resistance against $1000/T$. Ideally, a linear line in this plot indicates activated transport. As one can notice, each curve shows non-linear behavior, where the high temperature region is linear, and at low temperatures deviates from the linear behavior.

3. Results and discussion

3.1. Electrical transport measurements

We measured the resistance R of the samples as a function of temperature T in the range between 1.5–200 K. We applied gate voltage (V_g) to the side gate in contact with ionic liquid at 260 K and subsequently the sample was cooled at a fixed V_g . Below 220 K, the ionic liquid freezes out completely and stable electrical measurements become possible. The gate modulation was achieved in the range of -2 V to 3 V, without significant degradation of samples. V_g applied outside of this regime caused electrochemical reactions, resulting in irreproducible $R(T)$. Figure 1 (a) shows $R(T)$ for SIO films doped

chemically with La (filled symbols) and undoped samples using an ionic liquid gate (open symbols). All samples exhibit $dR/dT < 0$, i.e. an insulating behavior, regardless of chemical doping (up to 10% La doping).

The resistance of ionic liquid gated sample changes rapidly with decreasing T , whose behavior can be modulated by V_g . To quantify this gate dependence, we replot $R(T)$ as a function of V_g at three different temperatures such as 250 K, 200 K and 150 K. (shown in figure 1(b)). As one can see, the application of negative V_g leads to accumulation of carriers (p-type, as shown below using Hall measurements), and hence, lower $R(T)$ compared to the undoped state. Positive V_g leads to depletion, which is signalled by the saturation of the resistance, and eventually, we achieve inversion with increasingly positive V_g . Due to the limitation on the V_g range from electro-chemical reactions, we were not able to achieve complete inversion. As we show in the subsequent discussions, ionic liquid gating leads to relatively milder changes in the Hall mobility as compared to sheet resistance (as shown in figure 2(b)), hence the shown evolution of resistance with V_g indicates possible ambipolar transport in SIO. Previously, demonstration of ambipolar doping in a Mott insulator was realized only by chemical doping across many samples [26]. In our experiment, we have attempted to show ambipolar doping of a Mott insulator (SIO) in a single sample via electrochemical modulation. Ideally ambipolar transport behavior can be confirmed by accompanying Hall measurements. However high resistivity in the sample with low carrier density made it difficult to perform a reliable Hall measurement. Further evidence for the ambipolarity in this system using the Hall measurements in heavily doped SIO shall be discussed subsequently. One must be careful in interpreting such an evolution of resistance with gate voltage. The presence of impurity bands, due to defects such as oxygen vacancies and cationic disorder, can complicate the interpretation related to chemical potential tuning across the Mott gap.

The temperature dependence of these samples can be qualitatively divided into two regimes (as shown in the inset of figure 1(b)): (i) high temperature activated regime ($T \gtrsim 150$ K), where $R(T)$ follows an activated (Arrhenius) behavior; and (ii) low temperature variable range hopping regime ($T \lesssim 150$ K), where $R(T)$ deviates from the Arrhenius behavior and exhibits hopping conduction. As the temperature range under question for both these regimes are too small to make accurate and quantitative determination of this regime change, we make qualitative estimate of this crossover. Further discussions on the nature of conduction will follow after we understand the effect of gating on the conductance of the SIO films.

3.2. Effect of ionic liquid gating on film conductance

In order to understand the nature of the gated surface layer, we used a simple two layer model as depicted in the lower inset of figure 2(a). Hall measurements show that the undoped bulk sample has a weak p-type doping (figure 2(b)), with a carrier density $n \approx 2.5 \times 10^{14} \text{ cm}^{-2}$. Upon electrolyte gating, EFE induced charges accumulate on the surface layer, which

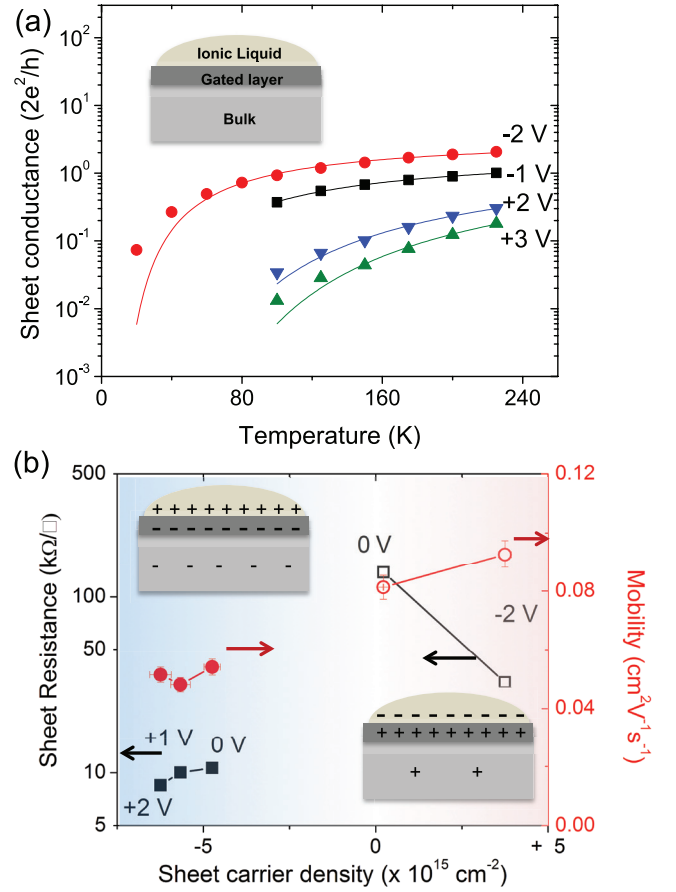


Figure 2. (a) Temperature dependent sheet conductances of the ionic liquid gated surface layers measured at different gate voltages (from figure 1(b)). The conductance of the surface layer ΔG was obtained by subtracting the conductance of the ungated portion of the samples (see the inset for a schematic bi-layer model). The solid lines are fits using activation to the mobility edge (see text). (b) Gate modulated sheet resistance (black squares) and Hall mobility (red circles) for a 10 nm thick 10% La doped SIO thin film (filled symbols) and a 25 nm thick undoped SIO thin film (open symbols) as a function of the Hall sheet carrier density (modulated by the gate voltage). The data were obtained at similar temperatures of 190 and 150 K respectively. The inset shows the schematic diagram of free and bound charge distributions in the samples.

has different conductivity as compared to the bulk of the film. Figure 2(b) clearly shows that one can achieve n-type and p-type carriers using chemical and EFE doping respectively. This establishes ambipolar transport behavior in doped SIO system, while we cannot completely rule out the influence of impurity induced band formation. For the hole accumulation side ($V_g < 0$), the conductance of the surface layer, G_s , can be estimated from the difference of the conductance with reference to $R_0 = R(V_g = 0 \text{ V})$: $G_s(V_g) = R(V_g)^{-1} - R_0^{-1}$.

In the case of electron doping ($V_g > +1$), a depletion layer is formed first on the surface and then gradually becomes electron doped (n-type) for higher V_g . Therefore $R(V_g)$ increases initially when V_g increases as shown in figure 1(a) and then starts decreasing for higher V_g . For undoped samples, $R(V_g)$ is the largest for $V_g \approx +1 \text{ V}$. The thickness of depletion layer, ℓ_d , thus can be estimated from $\ell_d = (R(V_g = +1 \text{ V})/R_0 - 1)d \approx 4 \text{ nm}$, where $d = 10 \text{ nm}$ is the thickness of the sample. Using

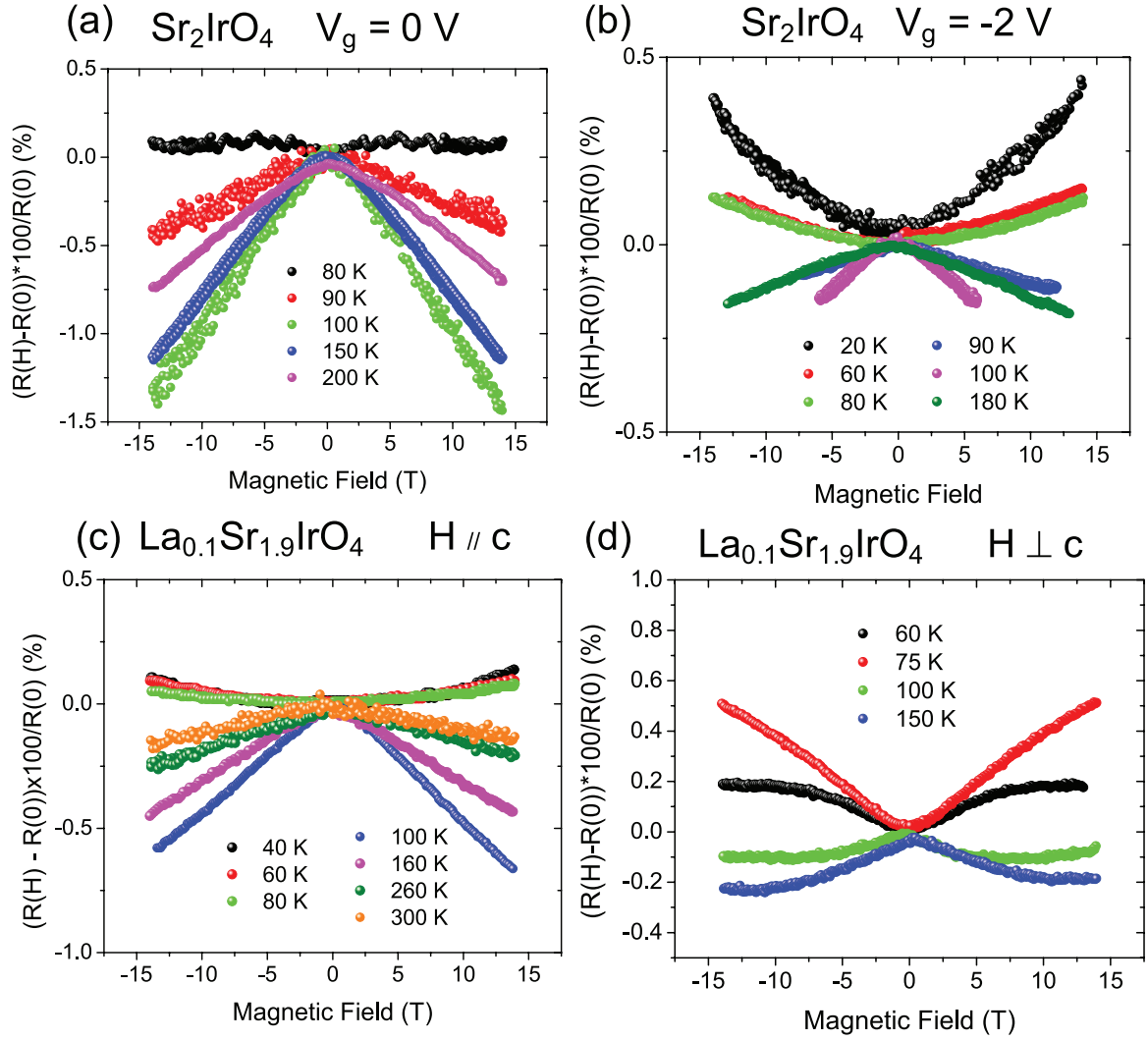


Figure 3. The measured MR as a function of both applied magnetic field and temperature for (a) undoped SIO, (b) ionic liquid gated SIO (hole doped with $V_g = -2$ V), (c) electron doped $\text{La}_{0.1}\text{Sr}_{1.9}\text{IrO}_4$ thin film, and (d) electron doped $\text{La}_{0.1}\text{Sr}_{1.9}\text{IrO}_4$ thin film with applied field parallel to the a - b plane. For all the other three cases, except (d), the magnetic field was applied parallel to c -axis.

ℓ_d , we can estimate G_s for this inversion regime by subtracting the sheet conductance of the depleted layer using : $G_s = R(V_g)^{-1} - \left(\frac{d - \ell_d}{d}\right) R_0^{-1}$. Figure 2(a) shows $G_s(T)$ for fixed V_g . The conductance steeply drops as T decreases, which is expected from the transport through localized states.

We employ a simple activation model to mobility edge to describe the temperature dependent transport through the surface conduction layer: $G_s = G_{\min} \exp\left[\frac{-(E_{\text{ME}} - E_F)}{k_B T}\right]$, where E_{ME} , E_F , and G_{\min} are the mobility edge, Fermi energy, and Mott minimum conductance, respectively. Typically such an analysis is performed on semiconductors, which exhibit disorder induced mobility edge [27], where characteristic carrier density and temperature dependence of the mobility is observed. Using this simple activation formula, we fit the experimental data of temperature dependent G_s for fixed V_g (solid lines in figure 2(a)). The activation fits are reasonable for most of gate voltages at higher temperature ranges ($T \gtrsim 150$ K), but starts deviating at lower temperatures, likely indicating the limitations of such a model at low temperatures. The obtained

values of G_{\min} is $\sim \text{few } e^2/h$ with reasonable values for $\Delta E = E_{\text{ME}} - E_F$, as it is expected for 2D localization [28].

While the disorder driven localization theory seemingly explains the observed behavior of G_s , there are a few factors that are not captured by a simple localization theory. Figure 2(b) shows that the measured Hall mobility remains roughly constant ($\sim 0.08 \text{ cm}^2 \text{ Vs}^{-1}$), but we cannot attribute a definitive trend based on limited information available. This filling independent mobility is not expected for disorder induced localization, where one expects a steep increase of mobility as E_F is getting close to the mobility edge [27]. We also make a note on the strain effect on both the insulating state and the EFE on the transport properties. Although we have measured the transport properties of 25 nm thick SIO films on various substrates such as STO, LSAT, DSO (DyScO_3), and GSO (GdScO_3), which exert different amount of strain on SIO, the insulating nature of the material persists in all samples. Despite the qualitative similarity, the films showed subtle changes in the resistivity. There are a few reports on the effect of strain on the optical and transport gap of SIO in the literature [25, 29].

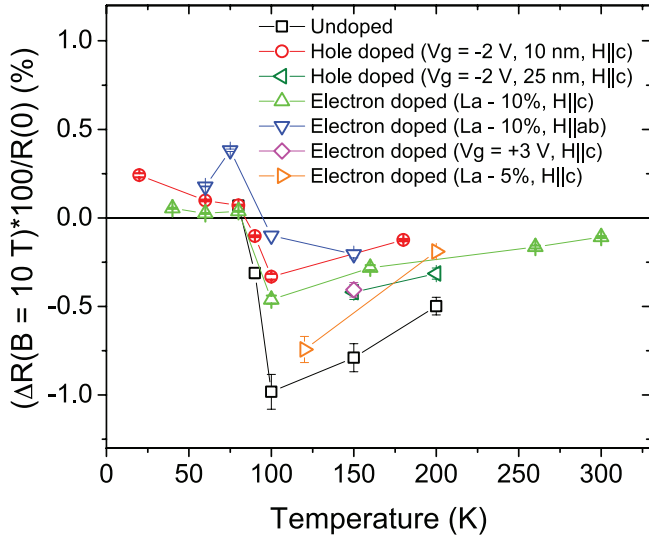


Figure 4. (a) The MR measured at the magnetic field of 10 T as a function of temperature for different n-type and p-type doping concentrations. The graph clearly highlights a MR crossover from negative to positive values at about ~ 80 – 90 K. The graph also shows high temperature negative MR for other doping (La 5%) and ionic liquid gated samples with different gate voltages used in this study.

3.3. Magneto-resistance in hopping conduction regime

The low temperature hopping regime can be dominated by either defect mediated hopping, known as Mott VRH [30] or by Coulombic interactions, known as Efros–Shklovskii (ES) VRH [31]. Temperature dependent VRH resistivity can be described by $\rho = \rho_0 \exp(T_0/T)^{1/\alpha}$, where T_0 is a characteristic hopping energy scale and α is the exponent, dependent on dimension and type of VRH [30, 31], where $\alpha = 4$ for Mott VRH and $\alpha = 2$ for ES VRH. While similar Mott-ES VRH crossover has been reported in undoped SIO [13], unfortunately, the temperature range in our experiment over which we have available resistance measurements is not sufficient to make an accurate determination of the nature of hopping transport in SIO thin film samples used in our study. Hence, in order to clarify the nature of the hopping conduction in SIO, we performed temperature dependent MR measurements.

MR has been studied extensively in the hopping conduction regime for several semiconductors and alloys [32–36], where the temperature and field dependence of MR has been used to explain the low temperature transport mechanism. Figure 3 shows the representative transverse MR for electron doped $\text{La}_{0.1}\text{Sr}_{1.9}\text{IrO}_4$ thin film (figure 3(a)), ionic liquid gated SIO (hole doped with $V_g = -2$ V) (figure 3(b)), electron doped $\text{La}_{0.1}\text{Sr}_{1.9}\text{IrO}_4$ thin film (figure 3(c)), and electron doped $\text{La}_{0.1}\text{Sr}_{1.9}\text{IrO}_4$ thin film with applied field parallel to the a – b plane (figure 3(d)). In all the above cases, the direction of the applied magnetic field was along the c -axis, unless otherwise specified. One can quickly notice that both electron and hole doped samples demonstrate an abrupt MR sign change at ~ 80 – 90 K, where based on qualitative temperature dependence, we can conclude that we are deep in the hopping transport regime. At low temperatures, the MR exhibits a positive, quadratic scaling with the magnetic field, but at high

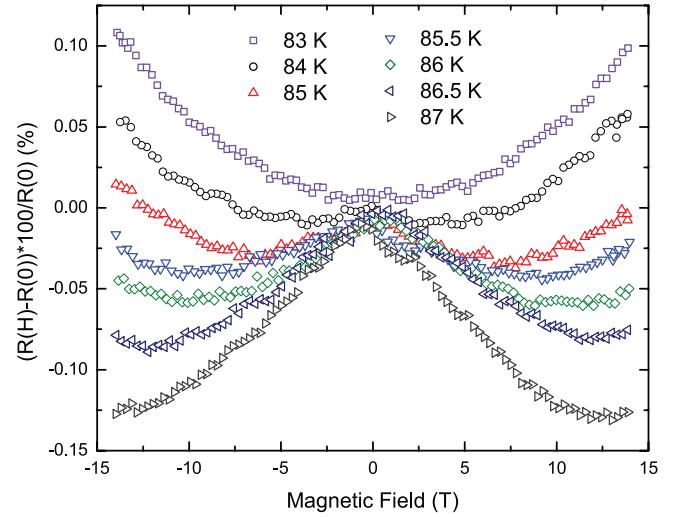


Figure 5. The MR measured as a function of the magnetic field at different temperatures (83–87 K) right around the MR sign change for the electron doped $\text{La}_{0.1}\text{Sr}_{1.9}\text{IrO}_4$ thin film (shown in figure 3(a)). The graph clearly highlights a MR crossover from negative to positive values, which is sensitively dependent on both the magnetic field and temperature.

temperatures, the MR shows a negative, linear scaling with the magnetic field.

To clearly establish the universality of the MR crossover, in figure 4, we show the variation of MR at an applied field of 10 T. This plot highlights the experimental observation that the MR sign change is qualitatively similar for a variety of filling (both n-type and p-type). Although the magnitudes of MR are quite different, interestingly, the MR sign change appears in all of our samples with nearly similar crossover temperature $T_{cr} \sim 80$ – 90 K. Similar temperature dependent MR behavior was reported in highly compensated n-GaAs [34], and more recently in undoped SIO [15], further suggesting the qualitative similarities of MR crossover in these systems. In order to resolve the finer details of this transition near the crossover, we performed MR measurements on electron doped $\text{La}_{0.1}\text{Sr}_{1.9}\text{IrO}_4$ thin film with smaller temperature intervals. Figure 5 shows the field and temperature dependent MR crossover in 10% La doped samples over a narrow range of temperatures from 83–87 K. This behavior is strikingly similar (qualitatively) to the MR crossover reported in hopping regime of several disordered semiconductors and alloys [32–36]. Although this MR crossover in SIO has qualitative similarities to the MR crossover observed in compensated semiconductors, the magnitude of MR and temperature range over which this crossover occurs a very different in both the systems. This limits our ability to directly employ the explanations used for the MR crossover in these compensated semiconductors [32–36].

3.4. Magnetization measurements on doped and undoped SIO

Before we discuss the interpretation of the MR results, it is necessary to understand the magnetization behavior in SIO. As SIO undergoes a paramagnetic to antiferromagnetic transition

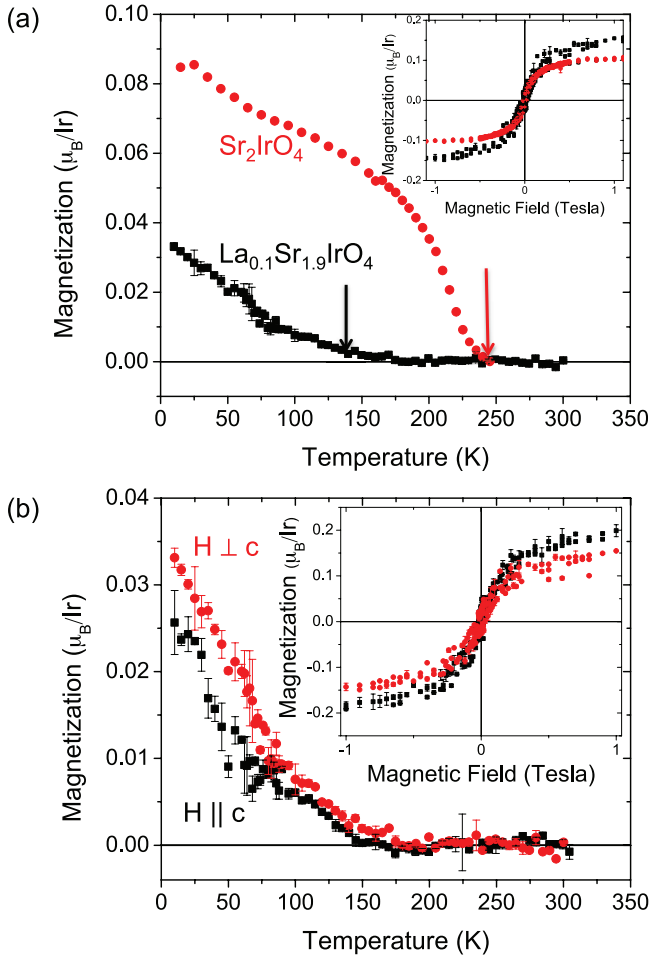


Figure 6. (a) The measured field cool magnetization values as a function of temperature for Sr_2IrO_4 (red circles at applied field = 0.8 T) and $\text{La}_{0.1}\text{Sr}_{1.9}\text{IrO}_4$ (black squares at applied field = 0.5 T). The plot clearly shows a ferromagnetic transition for Sr_2IrO_4 at 240 K and $\text{La}_{0.1}\text{Sr}_{1.9}\text{IrO}_4$ at ~ 130 – 140 K. The inset shows a ferromagnetic hysteresis loop for both the cases. The magnetic field was applied along the a - b plane. (b) The measured field cool magnetization values for $\text{La}_{0.1}\text{Sr}_{1.9}\text{IrO}_4$ with the magnetic field (0.5 T) applied parallel to (i) the a - b plane (shown as red circles) and (ii) the c plane (shown as black squares). The inset shows the ferromagnetic hysteresis loop for both the cases. The graph clearly demonstrates the presence of little or no anisotropy. A constant diamagnetic background from the substrate (SrTiO_3) was subtracted to obtain the signal from the film in all the cases.

below room temperature, the MR behavior can be affected by the magnetic order in the system. In the case of SIO, it is well established that the antiferromagnetic state has a small canted moment, which can be used to study this magnetic transition [10, 16–18]. Hence, we performed in-depth magnetization measurements to compare the evolution of magnetic order and the magnetoresistance in SIO. Figure 6(a) shows the temperature dependent magnetization for both undoped and electron (10% La) doped SIO. We observe that the ferromagnetic transition temperature decreases from ~ 240 K to ~ 150 K upon electron doping. Below the magnetic transition, the magnetic field dependence of magnetization (inset figure) shows a well-developed spontaneous magnetization, suggesting the presence of long range magnetic order.

Figure 6(b) shows the magnetization measurements on electron (10% La) doped SIO for both transverse and longitudinal field. These measurements suggest that the magnetic order in these systems have little anisotropy within the measurement limitations of our magnetometry measurements unlike the MR measurements, which exhibit a stronger anisotropy. Similar results were obtained for nominally undoped SIO. We also note that the doping independent MR crossover occurs ~ 80 – 90 K, while the doping dependent magnetic order onset occurs ~ 240 – 150 K. Such a discrepancy in the temperature range for the magnetic transition and MR crossover strongly suggests that the magnetic order is likely not directly related to the MR crossover.

With the magnetization measurements in the backdrop, we can discuss the interpretation of the MR crossover. To understand the MR crossover, we first focus on understanding the limiting MR behavior. The high temperature linear negative MR in the VRH regime is often attributed to the quantum interference between the hops [37], which was experimentally observed in disorder semiconductors and quasicrystalline alloys [32, 33]. The low temperature positive MR can be attributed to several possibilities including the (i) the shrinking of electronic impurity wave function under a magnetic field [37]; (ii) spin dependent MR (Kamimura effect) [38] or (iii) superconducting or magnetic fluctuations [39]. We eliminate the role of superconducting fluctuations (i.e. (iii) above) as we are far from the metallic limit. We also exclude the possibility of a magnetic fluctuation based mechanism ((ii) above), since a decreasing MR with temperature is expected as we approach the ordering temperature. Moreover, as shown earlier, magnetization measurements on the undoped and 10% La doped samples exhibit a magnetic transition at ~ 240 K and ~ 150 K respectively, distinctly different from the filling independent MR crossover at ~ 80 – 90 K. Thus, we interpret the shrinking of the electronic impurity wave function as a probable cause for the observed positive MR at low temperatures.

With this limiting MR behavior in mind, one of the possible explanations for such an MR crossover behavior in disordered systems can often be associated with a Coulomb gap opening [35, 40, 41]. Further, such a crossover is expected to be band filling independent, as seen in our case [42]. On the other hand, SIO in single crystal form has been shown to demonstrate large magnetoelectric effect with anomalies in its dielectric constant and magnetization over a temperature range of 50–100 K [43]. It is likely that such anomalies and magneto-electric effect could be related to the observed magneto-resistance crossover. Further investigations are required to clarify the origin of these effects and their relationship.

4. Conclusions

In summary, we have demonstrated that ionic liquid gating can be used to realize ambipolar transport in thin films of SIO. Despite the large carrier injection, the insulating state persists for both electron and hole doping attainable in our experiments. We observe a robust MR sign change, around 90 K, irrespective of the filling, possibly signifying a temperature

dependent crossover behavior of underlying hopping transport mechanism.

Acknowledgments

This work was supported by U.S. National Science Foundation (NSF) via Grant DMREF Grant No. DMR-1435487, and the Penn State MRSEC, and by the SRC FENA-FAME program through UCLA. The work at Rutgers University was funded by the Gordon and Betty Moore Foundations EPiQS Initiative through Grant GBMF4413 to the Rutgers Center for Emergent Materials. We thank J T Heron for the help with magnetization measurements. The authors gratefully acknowledge several useful discussions with A Millis, I Aleiner, M Mueller, C Marianetti, J Liu and X Marti.

References

- [1] Brandow B H 1977 *Adv. Phys.* **26** 651
- [2] Imada M, Fujimori A and Tokura Y 1998 *Rev. Mod. Phys.* **70** 1039
- [3] Klein Y and Terasaki I 2008 *J. Phys.: Condens. Matter* **20** 295201
- [4] Haskel D, Fabbri G, Zhernenkov M, Kong P P, Jin C Q, Cao G and van Veenendaal M 2012 *Phys. Rev. Lett.* **109** 027204
- [5] Kim B J *et al* 2008 *Phys. Rev. Lett.* **101** 076402
- [6] Moon S J, Jin H, Choi W S, Lee J-S, Seo S S A, Yu J, Cao G, Noh T W and Lee Y S 2009 *Phys. Rev. B* **80** 195110
- [7] Hsieh D, Mahmood F, Torchinsky D H, Cao G and Gedik N 2012 *Phys. Rev. B* **86** 035128
- [8] Dai J, Calleja E, Cao G and McElroy K 2014 *Phys. Rev. B* **90** 041102
- [9] Li Q *et al* 2013 *Sci. Rep.* **3** 3073
- [10] Cao G, Bolivar J, McCall S, Crow J E and Guertin R P 1998 *Phys. Rev. B* **57** R11039
- [11] Korneta O B, Qi T, Chikara S, Parkin S, De Long L E, Schlottmann P and Cao G 2010 *Phys. Rev. B* **82** 115117
- [12] Lee J-S, Krockenberger Y, Takahashi K S, Kawasaki M and Tokura Y 2012 *Phys. Rev. B* **85** 035101
- [13] Lu C, Quindeau A, Deniz H, Preziosi D, Hesse D and Alexe M 2014 *Appl. Phys. Lett.* **105** 082407
- [14] Wang C, Seinige H, Cao G, Zhou J-S, Goodenough J B and Tsoi M 2015 *J. Appl. Phys.* **117** 17A310
- [15] Lu C, Dong S, Quindeau A, Preziosi D, Hu N and Alexe M 2015 *Phys. Rev. B* **91** 104401
- [16] Boseggia S, Springell R, Walker H C, Ronnow H M, Rüegg C, Okabe H, Isobe M, Perry R S, Collins S P and McMorro D F 2013 *Phys. Rev. Lett.* **110** 117207
- [17] Kim J *et al* 2012 *Phys. Rev. Lett.* **108** 177003
- [18] Fujiyama S, Ohsumi H, Komesu T, Matsuno J, Kim B J, Takata M, Arima T and Takagi H 2012 *Phys. Rev. Lett.* **108** 247212
- [19] Wang F and Senthil T 2011 *Phys. Rev. Lett.* **106** 136402
- [20] Ahn C, Bhattacharya A, Di Ventura M, Eckstein J, Frisbie C, Gershenson M, Goldman A, Inoue I, Mannhart J and Millis A 2006 *Rev. Mod. Phys.* **78** 1185
- [21] Misra R, McCarthy M and Hebard A F 2007 *Appl. Phys. Lett.* **90** 052905
- [22] Ueno K, Nakamura S, Shimotani H, Yuan H T, Kimura N, Nojima T, Aoki H, Iwasa Y and Kawasaki M 2011 *Nat. Nanotechnol.* **6** 408
- [23] Leng X, Garcia-Barriocanal J, Bose S, Lee Y and Goldman A M 2011 *Phys. Rev. Lett.* **107** 027001
- [24] Bollinger A T, Dubuis G, Yoon J, Pavuna D, Misewich J and Bozovic I 2011 *Nature* **472** 458
- [25] Rayan Serrao C *et al* 2013 *Phys. Rev. B* **87** 085121
- [26] Segawa K, Kofu M, Lee S-H, Tsukada I, Hiraka H, Fujita M, Chang S, Yamada K and Ando Y 2010 *Nat. Phys.* **6** 579
- [27] Arnold E 1974 *Appl. Phys. Lett.* **25** 705
- [28] Tsui D and Allen S 1974 *Phys. Rev. Lett.* **32** 1200
- [29] Nichols J, Terzic J, Bittle E G, Korneta O B, De Long L E, Brill J W, Cao G and Seo S S A 2013 *Appl. Phys. Lett.* **102** 141908
- [30] Mott N F 1969 *Phil. Mag.* **19** 835
- [31] Efros A L and Shklovskii B I 1975 *J. Phys. C: Solid State Phys.* **8** L49
- [32] Zhang Y, Dai P and Sarachik M P 1992 *Phys. Rev. B* **45** 9473
- [33] Srinivas V, Rodmar M, Poon S J and Rapp Ö 2001 *Phys. Rev. B* **63** 172202
- [34] Rentzsch R, Ionov A N, Sandow B, Stefanyi P, Fozooni P and Lea M J 1997 *Phys. Status Solidi b* **203** 487
- [35] Agrinskaya N V, Kozub V I and Shamshur D V 1995 *J. Exp. Theor. Phys.* **80** 1142
- [36] Rosenbaum R, Murphy T, Palm E, Hannahs S and Brandt B 2001 *Phys. Rev. B* **63** 094426
- [37] Nguen V L, Spivak B Z and Shklovskii B I 1985 *Zh. Eksp. Teor. Fiz.* **89** 1770
- [38] Kamimura H, Kurobe A and Takemori T 1983 *Physica B + C* **117-8** 652
- [39] Maki K 1968 *Prog. Theor. Phys.* **40** 193
- [40] Agrinskaya N V, Kozub V I, Shumilin A V and Sobko E 2010 *Phys. Rev. B* **82** 075201
- [41] Agrinskaya N V, Kozub V I, Rentzsch R, Lea M J and Fozooni P 1997 *J. Exp. Theor. Phys.* **84** 814
- [42] Davies J H and Franz J R 1986 *Phys. Rev. Lett.* **57** 475
- [43] Chikara S, Korneta O B, Crummett W, De Long L E, Schlottmann P and Cao G 2009 *Phys. Rev. B* **80** 140407